

Serveur Académique Lausannois SERVAL [serval.unil.ch](http://serval.unil.ch)

## Author Manuscript

Faculty of Biology and Medicine Publication

This paper has been peer-reviewed but does not include the final publisher proof-corrections or journal pagination.

Published in final edited form as:

**Title:** Targeted  $\gamma$ -secretase inhibition of Notch signaling activation in acute renal injury.

**Authors:** Wyss JC, Kumar R, Mikulic J, Schneider M, Aebi JD, Juillerat-Jeanneret L, Golshayan D

**Journal:** American journal of physiology. Renal physiology

**Year:** 2018 May 1

**Issue:** 314

**Volume:** 5

**Pages:** F736-F746

**DOI:** 10.1152/ajprenal.00414.2016

In the absence of a copyright statement, users should assume that standard copyright protection applies, unless the article contains an explicit statement to the contrary. In case of doubt, contact the journal publisher to verify the copyright status of an article.

1 **Revised manuscript**

2 **Targeted gamma-secretase inhibition of Notch signaling activation in acute**  
3 **renal injury**

4  
5 Jean-Christophe Wyss<sup>1</sup>, Rajesh Kumar<sup>1,4</sup>, Josip Mikulic<sup>1</sup>, Manfred Schneider<sup>2</sup>, Johannes D  
6 Aebi<sup>2</sup>, Lucienne Juillerat-Jeanneret<sup>1,3</sup>, Dela Golshayan<sup>1,\*</sup>.

7  
8 <sup>1</sup> Transplantation Center and Transplantation Immunopathology Laboratory, Department of  
9 Medicine, Centre Hospitalier Universitaire Vaudois (CHUV) and University of Lausanne  
10 (UNIL), Lausanne, Switzerland

11 <sup>2</sup> Medicinal Chemistry, Roche Pharma Research and Early Development (pRED), Roche  
12 Innovation Center, F. Hoffmann-La Roche Ltd, CH-4070 Basel, Switzerland

13 <sup>3</sup> University Institute of Pathology, CHUV and UNIL, Lausanne, Switzerland

14 <sup>4</sup> current address: Surgical Oncology Research Lab, Massachusetts General Hospital, Harvard  
15 Medical School, Boston MA, USA

16  
17 *Running head:* Notch inhibition in kidney diseases

18 \***Corresponding author:** PD Dr D Golshayan MD PhD, Transplantation Centre, CHUV,  
19 Bugnon 46, 1011 Lausanne, Switzerland.

20 Phone: +41 795564762; Fax: +41 213141175; Email: [Dela.Golshayan@chuv.ch](mailto:Dela.Golshayan@chuv.ch)

21  
22 *Contribution of authors:* LJJ and DG designed the project, evaluated the results and wrote the  
23 manuscript; JDA participated in the design of the project, designed and prepared the  
24 compounds and participated in the evaluation of the results and the writing of the manuscript;  
25 MS designed, performed and evaluated the pharmacokinetics data and participated in the  
26 writing of the manuscript; JCW, RK and JM performed the experiments, evaluated the results  
27 and participated in the writing of the manuscript.

28

29 **Abstract**

30 The Notch pathway has been reported to control tissue damage in acute kidney diseases. To  
31 investigate potential beneficial nephroprotective effects of targeting Notch, we developed  
32 chemically functionalized  $\gamma$ -secretase inhibitors (GSIs) targeting  $\gamma$ -glutamyltranspeptidase ( $\gamma$ -  
33 GT) and/or  $\gamma$ -glutamylcyclotransfase ( $\gamma$ -GCT), two enzymes overexpressed in the injured  
34 kidney, and evaluated them in *in vivo* murine models of acute tubular and glomerular damage.  
35 Exposure of the animals to disease-inducing drugs together with the functionalized GSIs  
36 improved proteinuria and, to some extent, kidney dysfunction. The expression of genes  
37 involved in the Notch pathway, acute inflammatory stress responses and the renin-angiotensin  
38 system was enhanced in injured kidneys, which could be downregulated upon administration  
39 of functionalized GSIs. Immunohistochemistry staining and western blots demonstrated  
40 enhanced activation of Notch1 as detected by its cleaved active intracellular domain during  
41 acute kidney injury, and this was down-regulated by concomitant treatment with the  
42 functionalized GSIs. Thus, targeted  $\gamma$ -secretase-based prodrugs developed as substrates for  $\gamma$ -  
43 GT/ $\gamma$ -GCT have the potential to selectively control Notch activation in kidney diseases with  
44 subsequent regulation of the inflammatory stress response and the renin-angiotensin  
45 pathways.

46

47 **Key words:**  $\gamma$ -secretase inhibitors / Notch /  $\gamma$ -glutamyltranspeptidase ( $\gamma$ -GT) / aminopeptidase  
48 A / kidney diseases / renin-angiotensin / drug-targeting

49

50 Words count (with references, without abstract and figure legends): 5947

## 51 **Introduction**

52 Recent advanced knowledge on acute and chronic renal injury has yielded several common  
53 candidate pathways for designing targeted therapeutics, which include the Notch pathway, the  
54 oxidative stress response and the renin-angiotensin system (RAS) (3,20,21,31,42). The Notch  
55 pathway is a target for therapeutic intervention, not only in kidney diseases but also in several  
56 other disorders (20,36). Notch is a membrane inserted protein with its active part directed  
57 toward the intracellular space and which needs hydrolysis by the  $\gamma$ -secretase complex to  
58 become active (20). The enzyme  $\gamma$ -secretase is a large protease complex composed of a  
59 catalytic aspartyl protease subunit (presenilin-1 or -2) and three support subunits (presenilin  
60 enhancer protein (pen)-2, aph-1 and nicastrin), all being membrane-inserted proteins. The  $\gamma$ -  
61 secretase complex activates Notch by hydrolyzing a peptide bond of the Notch protein at an  
62 intra-membrane site, allowing cleaved Notch, also referred to as Notch intracellular domain  
63 (NICD), to migrate to the nucleus where it activates responsive genes (45). The intra-  
64 membrane activity of the  $\gamma$ -secretase has also been involved in the release from the membrane  
65 of other biologically relevant membrane proteins involved in physiological and pathological  
66 processes, including amyloid precursor protein, LDL-receptors, insulin-like growth factor or  
67 CD44. Therefore, in order to develop selective therapies for kidney diseases involving the  
68 control of Notch activation, it is desired to achieve only localized  $\gamma$ -secretase inhibition, thus  
69 protecting the other functions of this enzyme and of the Notch pathway in non-target organs.

70

71 Toward this goal and based on our previous knowledge that the activities of the peptidases  $\gamma$ -  
72 glutamyltranspeptidase ( $\gamma$ -GT) and aminopeptidase A (APA) are increased in various  
73 compartments of injured kidneys in rodent experimental models as well as in human samples,  
74 we have designed, synthesized and evaluated targeted  $\gamma$ -secretase inhibitors (GSIs) as prodrug  
75 substrates for these enzymes (17). Preliminary *in vivo* results suggested the possibility of the

76 approach of using targeted GSIs in an experimental model of acute kidney injury. However,  
77 in our previous report, the biological consequences of exposing the animals to these targeted  
78 compounds and the *in vivo* effects on the expression of the components of the Notch pathway  
79 and other associated cellular responses were not studied. Thus in the present report, these  
80 functionalized  $\gamma$ -secretase-based prodrugs were evaluated in the experimental murine model  
81 of severe acute tubulointerstitial injury induced by aristolochic acid (AA) and the more  
82 progressive model of glomerular damage after exposure to adriamycin (ADR). Control and  
83 treated animals were monitored throughout the experiments for weight, proteinuria and  
84 relevant serum chemistry values. The toxicological profile of the N-acetyl- $\gamma$ -Glu- $\gamma$ -secretase-  
85 inhibitor (N-Ac- $\gamma$ -Glu-GSI) prodrug and its metabolite amine-GSI was determined in the  
86 plasma. To investigate the potential biological consequences of exposing the animals to these  
87 various compounds, we used real-time quantitative PCRs performed on mRNA extracted  
88 from the kidneys of the experimental animals as well as immunohistology and western  
89 blotting. The results demonstrated an activation of Notch1 with upregulation of the expression  
90 of genes involved in the Notch pathway, inflammatory stress response and the RAS, which  
91 could be selectively down-regulated upon administration to the mice of the N-Ac- $\gamma$ -Glu-GSI  
92 and/or its active metabolite amine-GSI, together with selective inhibition of Notch cleavage.

93

## 94 **Materials and Methods**

### 95 *Animal models of induced kidney injury*

96 All experiments were conducted in accordance with federal and local regulations, according  
97 to a protocol approved by the animal ethics committee of the Canton de Vaud, Switzerland  
98 (permit No 2655.0). Kidney injury was induced by intraperitoneal (i.p.) injection of  
99 aristolochic acid (AA, Sigma-Aldrich, Buchs, Switzerland, 1x5 mg/kg) or of adriamycin  
100 (Adriblastin, Pfizer, Zürich, Switzerland, 1x10 mg/kg) in 10 weeks old BALB/c male mice  
101 (n=5-7 mice/experimental group). The  $\gamma$ -secretase inhibitors (GSIs) compounds were diluted  
102 in 0.9% NaCl and administered i.p., starting one day before the disease-inducing drugs (day -  
103 1) at a dose of 10 mg/kg for amine-GSI or 30 mg/kg for N-Ac- $\gamma$ -Glu-GSI, and then twice  
104 daily until day 6 evening. A control group received the GSIs prodrugs without induction of  
105 kidney injury. The animals were weighted at days 0, 3 and 6, and sacrificed at day 7 morning.  
106 Proteinuria was assessed semi-quantitatively using Albustix reagent strips (Bayer, Basel,  
107 Switzerland). At the end of the treatment period, the mice were sacrificed, and the liver and  
108 both kidneys were removed. The kidneys were spliced in four equal fragments containing  
109 equivalent amounts of cortex and medulla. One fragment was snap-frozen in liquid nitrogen  
110 for qRT-PCR and western blot experiments, one fragment was included in OCT (Tissue-Tek,  
111 VWR International, Dietikon, Switzerland) and frozen for histoenzymography and  
112 immunohistochemistry experiments, one fragment was frozen at -80°C and was used to  
113 quantify drugs, and one fragment was fixed in 4% paraformaldehyde and included in paraffin  
114 for histology. Hematoxylin/eosin (HE) and Masson's trichrome blue (MTB) stainings of  
115 paraffin-embedded mouse kidney sections were performed using standard routine procedures.  
116 Blood samples were collected in tubes containing EDTA, plasma was separated by  
117 centrifugation and stored at -80°C. The clinical blood chemistry evaluation (kidney and liver  
118 function tests) in mouse plasma was performed according to standard procedures.

119 ***Immunohistochemistry***

120 OCT-embedded frozen kidneys were cut at 7  $\mu$ m. The sections were air-dried, fixed for 10  
121 min in cold (-20 °C) methanol, rinsed in PBS 0.1% Triton X-100 (PBS/Triton), and blocked  
122 for 30 min with PBS/Triton containing 5% bovine serum albumin (BSA). Endogenous  
123 peroxidase and biotin were blocked using 3% H<sub>2</sub>O<sub>2</sub> and avidin/biotin blocking kit (Vector  
124 Laboratories, Burlingame, CA 94010, USA), respectively. The rabbit anti-Notch1 antibody  
125 (clone D1E11, Cell Signaling Technology, Leiden, The Netherland; diluted 1/50 in PBS/5%  
126 BSA) or the rabbit anti-cleaved Notch1 antibody (clone Val1744, Cell Signaling; diluted 1/50  
127 in PBS/5% BSA) were added to the sections for 1 h. The slides were rinsed with PBS/Triton  
128 three times, incubated for 1 h with biotinylated anti-rabbit secondary antibody (Vector  
129 Laboratories, diluted 1/500 in PBS/5% BSA), washed with PBS, incubated with  
130 streptavidin/horse radish peroxidase (HRP) (Dako, Bollscheil, Germany; diluted 1/500) for  
131 1 h, followed by 15 min with 3,3'-diaminobenzidine (DAB, Dako). The slides were washed in  
132 distilled water, mounted in Aquamount, (Immu-mount, Thermo Shandon Pittsburgh, PA,  
133 USA) and analyzed.

134 For the staining of  $\alpha$ -smooth muscle actin ( $\alpha$ -SMA), paraffin-embedded kidney sections were  
135 used. Slides were deparaffined following standard procedures and endogenous peroxidase was  
136 blocked using 1% H<sub>2</sub>O<sub>2</sub> in methanol. Slides were then rehydrated by washing in decreasing  
137 gradients of ethanol (100% twice, 95% twice, 80% once) followed by tap water, then blocked  
138 10 min in PBS/10% goat serum before adding the primary antibody for 1 h (rabbit anti- $\alpha$ -  
139 SMA, Abcam; diluted 1/200 in PBS-0.1% BSA), followed by anti-rabbit HRP and DAB. The  
140 slides were rinsed in tap water and briefly counterstained with Harris hematoxyline. For NF $\kappa$ B  
141 p65, the same protocol was applied with an added antigen retrieval step using citrate buffer  
142 pH 6 and heating in microwave, before adding the primary antibody (rabbit anti-NF $\kappa$ B p65,  
143 GeneTex; diluted 1/1000 in PBS/0,1% BSA).

144 ***Real-time quantitative PCR (qRT-PCR)***

145 Total RNA was extracted from frozen kidney fragments of either untreated mice or mice  
146 treated with the various drugs (n=5-7 mice per experimental group), using the TRIzol reagent  
147 (Life Technologies, USA) as per the manufacturer's instructions. Briefly, 10mg of kidney  
148 sample was homogenized using a polytron (VWR International). The nucleic acids were  
149 purified by chloroform/isopropanol extraction, quantified with the NanoDrop-ND2000  
150 (Thermo Scientific, USA) and treated by DNase (Promega, USA). DNase-treated RNA  
151 samples (260/280 nm absorbance ratio of 1.9-2.0) were subjected to cDNA synthesis with the  
152 iScript<sup>TM</sup> cDNA Synthesis Reverse Transcription (RT) kit (Bio-rad Laboratories, USA) as per  
153 the manufacturer's instructions. For gene expression profiling, SYBR Green (SensiMix<sup>TM</sup>  
154 SYBR kit, Quantace)-based qPCRs were performed for quantification of a particular  
155 transcript using specific primers with Rotor-Gene 6000 instrument (Corbett Research,  
156 Australia). Intron spanning and exon-specific primers were designed and synthesized by  
157 Microsynth, Switzerland. The sequences of the primers used are provided in **Table 1**.  
158 Standard curve analysis (>80% efficiency with single melting curve) was performed to  
159 validate the primers and PCR amplicons checked on ethidium bromide-containing agarose  
160 gels. To calculate the relative changes in mRNA expression, the ddCt method (**25**) was used.  
161 Gene expression levels were normalized to *Gapdh* and the control (vehicle-treated) animal  
162 group was assigned 100%. The levels of expression of interleukin (IL)-1 $\beta$ , IL-6, nuclear  
163 factor-kappa (NF $\kappa$ )B1 and NF $\kappa$ B2, Notch1, hairy and enhancer of split-1 (Hes1), Neph1n1,  
164 Snail, cyclin-dependent kinase (CDK)2, angiotensinogen (AGT), renin, APA and angiotensin  
165 receptor 1 (AT1) mRNAs were quantified by qRT-PCR and averaged for all animals.

166

167 ***Western blots***



168 Frozen mice kidneys were homogenized using a polytron in RIPA lysis buffer (150mM  
169 sodium chloride, 1% NP-40, 0.5% sodium deoxycholate, 0.1% SDS, 50mM Tris, pH 8.0,  
170 complete-EDTA free protease inhibitor cocktail (Roche, Germany)) and centrifuged for 20  
171 min (13000g) at 4°C. Tissue lysates were separated by SDS-PAGE and proteins transferred to  
172 PVDF membrane (Bio-Rad, USA). Following transfer, the membranes were probed with  
173 rabbit anti-cleaved Notch1 antibody (clone Val1744; diluted 1:1000) overnight at 4°C. After  
174 washing, blots were incubated for 1 h with a secondary anti-rabbit HRP antibody (dilution  
175 1:1000, Cell Signaling Technology) at room temperature. Blots were probed with an anti-  
176 GAPDH antibody (clone 14C10, Cell Signaling Technology; diluted 1:1000) as a loading  
177 control. Membranes were developed using Pierce ECL Plus (Thermo Scientific, USA). Bands  
178 intensities were quantified using Image J and presented as relative expression to the loading  
179 control (GAPDH).

180

### 181 *Statistical analysis*

182 The level of statistical significance between multiple experimental groups was assessed using  
183 one-way analysis of variance (ANOVA) along with Tukey's post-test for multiple  
184 comparisons (GraphPad Prism version 6, California). P values <0.05 were considered  
185 significant (\*p<0.05, \*\*p<0.01, \*\*\*p <0.001).

## 186 **Results**

### 187 *Effects of the functionalized GSIs in the aristolochic acid-induced murine model of acute* 188 *tubulointerstitial injury*

189 The chemical structures of the compounds used here are shown in **Figure 1**. Previous *in vitro*  
190 and *ex vivo* experiments (**17**) had demonstrated the cleavage of the inactive prodrug N-Ac- $\gamma$ -  
191 Glu-GSI resulting in the release of the active amine-GSI in the presence of the enzymes  $\gamma$ -  
192 GT/ $\gamma$ -GCT, while no further hydrolysis to the free inhibitor occurred. Pharmacokinetic  
193 experiments, measuring the distribution of the N-Ac- $\gamma$ -Glu-GSI prodrug and its metabolite  
194 amine-GSI following i.p. administration in mice, had determined the optimal dose and mode  
195 of administration for these compounds (**17**). Using a preliminary *in vivo* setting, we could also  
196 demonstrate that the potent  $\gamma$ -secretase inhibitor amine-GSI was selectively liberated from the  
197 prodrug N-Ac- $\gamma$ -Glu-GSI in injured kidneys (**17**). Thus, the N-Ac- $\gamma$ -Glu-GSI prodrug and its  
198 amine-GSI metabolite were chosen to test selective kidney protection in the experiments  
199 described hereafter. To further investigate for potential beneficial nephroprotective effects of  
200 the compounds, firstly, the aristolochic acid (AA)-induced *in vivo* murine model of acute  
201 tubulointerstitial renal damage was selected. The efficacy and toxicity profile of the N-Ac- $\gamma$ -  
202 Glu-GSI prodrug and its metabolite amine-GSI in control and diseased animals was analyzed  
203 using standard clinical chemistry markers at day 7 after administration in our *in vivo* model  
204 (**Table 2**). The results showed that control mice treated with the N-Ac- $\gamma$ -Glu-GSI prodrug  
205 alone experienced no obvious toxicity other than a slight increase in liver enzymes values  
206 (mainly alanine aminotransferase, ALAT and aspartate aminotransferase, ASAT). AA  
207 treatment induced acute renal failure as evidenced by significant elevation of serum creatinine  
208 and urea levels. The addition of the N-Ac- $\gamma$ -Glu-GSI ameliorated kidney dysfunction, but did  
209 not allow complete prevention of acute tubulopathy induced by AA. Interestingly, AA had a  
210 moderate hepatotoxic effect (mainly cytolysis) which was also limited by the administration of

211 the prodrug, possibly due to upregulation of  $\gamma$ -GT in acutely injured hepatocytes.  
212 Administration of the amine-GSI i.e. the N-Ac- $\gamma$ -Glu-GSI prodrug metabolite directly yielded  
213 similar results.

214

215 Mice exposed to AA alone or treated with either the N-Ac- $\gamma$ -Glu-GSI or the metabolite  
216 amine-GSI were evaluated clinically (behavior, feeding) and their weight and level of  
217 proteinuria was measured at baseline (day 0), then at day 3 and 6 after administration of the  
218 various compounds (**Figure 2**). AA exposure induced severe weight loss, most probably due  
219 to decreased food and liquid intake (as determined by monitoring daily the food and drink  
220 stocks as well as cages beddings). While there was no significant beneficial effect of the GSIs  
221 analogs on weight loss during the 7 days follow-up, both drugs resulted in a remarkable  
222 improvement of proteinuria, already by day 3. Histological evaluation of the kidneys of the  
223 experimental mice confirmed the development of severe acute tubulointerstitial lesions after  
224 AA exposure (**Figure 3A**), which affected mainly the proximal tubules as previously  
225 described (**2**). The prodrug N-Ac- $\gamma$ -Glu-GSI given alone had no obvious deleterious effects on  
226 the liver and kidney architectures. In our experimental setting, the N-Ac- $\gamma$ -Glu-GSI treatment  
227 regimen could only partially prevent the severe tubulopathy induced by AA, corroborating the  
228 kidney function data. Despite the observed slight elevation of liver enzymes, the liver  
229 structure was mostly preserved in all experimental groups (**Figure 3B**). In our experimental  
230 model, mice were sacrificed on day 7, and besides the protective effect of the N-Ac- $\gamma$ -Glu-  
231 GSI prodrug on acute tubulointerstitial lesions, we also observed a decreased expression of  $\alpha$ -  
232 smooth muscle actin ( $\alpha$ -SMA) at this early time-point, suggesting a protective effect on the  
233 development of a profibrotic response following acute injury.

234

235 We next investigated specific local inhibition of the cleavage of Notch in the kidneys of

236 animals exposed to AA alone or in the presence of N-Ac- $\gamma$ -Glu-GSI (**Figure 4**).  
237 Immunohistochemistry stainings (**Figure 4A**) showed that while exposure to AA induced  
238 Notch1 expression and Notch1 cleavage reflecting Notch activation, treatment with the  
239 functionalized N-Ac- $\gamma$ -Glu-GSI significantly prevented the expression of cleaved Notch1. By  
240 itself and in the absence of AA-mediated injury, N-Ac- $\gamma$ -Glu-GSI had no effect on the  
241 cleavage of Notch in the kidney. These results were further confirmed by western blot analysis  
242 of cleaved Notch1 (also referred to as NICD) expression levels in control, AA-diseased and  
243 AA-diseased-N-Ac- $\gamma$ -Glu-GSI-treated kidney samples (**Figure 4B**). Finally, using  
244 histoenzymography, we further evaluated the effects of AA and the N-Ac- $\gamma$ -Glu-GSI on the  
245 activity of the target enzyme,  $\gamma$ -GT. At day 7 after AA exposure, kidneys of diseased mice  
246 were severely damaged so that we could not analyze any  $\gamma$ -GT activity at this late time-point  
247 nor illustrate, directly on tissue sections, the specific local activation of the GSI prodrug as  
248 substrate for this enzyme. However, in previous *ex-vivo* experiments, we were able to  
249 demonstrate early upregulation of the enzyme  $\gamma$ -GT mainly in proximal tubules of diseased  
250 kidneys and targeted activation of our prodrug allowing local inhibition of the hydrolytic  
251 cleavage of Notch (**17**). Overall, these data highlighted the protective effects but also the  
252 limitation of functionalized GSIs analogs, when used alone, in preventing severe acute  
253 tubulointerstitial injury such as in our *in vivo* model.

254

#### 255 ***Evaluation of downstream pathways associated with the inhibition of Notch1 cleavage***

256 At the end of the treatments (day 7), the animals were sacrificed and kidney sections were  
257 stored snap frozen for the determination by qRT-PCR of the mRNA levels of Notch1-  
258 responsive genes (**Figure 5A**, *Notch1*, *Nephrin1*, *HES1*, *Snail* and *CDK2*) and Notch1-  
259 inducible inflammatory genes (**Figure 5B**, *IL-1 $\beta$* , *IL-6*, *NF $\kappa$ B1* and *NF $\kappa$ B2*). By itself, the N-  
260 Ac- $\gamma$ -Glu-GSI did not induce the expression of genes of the Notch-dependent pathways.

261 Interestingly, compared to control animals, in animals exposed to AA, a significant induction  
262 of genes of the Notch downstream signaling pathway (*Notch1*, *Nephrin1*, *HES1*, *Snail*,  
263 *CDK2*) and of pro-inflammatory cytokines (*IL-1 $\beta$*  and *IL-6*) was observed, as well as an  
264 increased expression of genes encoding the transcription factors NF $\kappa$ B1 and NF $\kappa$ B2; all of  
265 which could be significantly reduced by concurrent treatment with N-Ac- $\gamma$ -Glu-GSI.  
266 Comparable information was obtained when analyzing kidneys of mice administered AA and  
267 the amine-GSI (data not shown). To further confirm these gene expression data on Notch-  
268 responsive genes and related inflammatory pathways, we investigated the expression of NF $\kappa$ B  
269 at the protein level; NF $\kappa$ B being one of the main regulators of cellular stress and inflammatory  
270 responses. As shown by immunohistochemistry on kidney sections (**Figure 5C**), while there  
271 was a high expression of NF $\kappa$ B p65 (active subunit of the NF $\kappa$ B transcription complex) in AA-  
272 injured kidneys, this expression was limited if the mice had also received the N-Ac- $\gamma$ -Glu-GSI  
273 treatment.

274

275 As dysfunction of the RAS has been involved in the development and/or progression of  
276 inflammatory disorders of the kidney, we also determined by qRT-PCR if modulation of the  
277 Notch pathway by GSIs, either the N-Ac- $\gamma$ -Glu-GSI or the amine-GSI, may also induce  
278 kidney-specific modifications in the expression of components of the RAS (**Figure 6**). In the  
279 RAS, the enzymes renin and angiotensin converting enzyme (ACE) sequentially hydrolyze  
280 the substrate angiotensinogen (AGT) to release the active octapeptide angiotensin (Ang) II  
281 able to bind to two functional receptors, AT1, which is the main receptor in the kidney, and  
282 AT2. Then the enzyme APA can hydrolyze the N-terminal Asp of Ang II, releasing Ang III,  
283 with different functions than Ang II. Thus, as APA is the main peptidase initiating the  
284 degradation of Ang II, we also evaluated this gene. Following AA administration to the mice,  
285 up-regulation of all the mRNAs evaluated for the RAS was observed, including the

286 expression of *APA* mRNA, suggesting a feed-back mechanism. However, the induction of  
287 *ATI* gene was low, and not always consistent between the experiments. Overall, these  
288 experiments demonstrated that the functionalized GSI prodrug was able to control, in part, the  
289 tissue stress response *in vivo* after severe acute kidney tubular injury by controlling the  
290 activation of the Notch pathway and its responsive genes downstream.

291

### 292 *Effects of the functionalized GSIs in the adriamycin-induced murine model of glomerular* 293 *injury*

294 The effect of the functionalized GSIs was also determined in another experimental model of  
295 renal disease induced by the administration of adriamycin (ADR). As opposed to AA which  
296 mainly induces acute tubulopathy, ADR administration is followed by progressive podocyte  
297 injury leading to glomerulosclerosis. Using human and mouse samples of diseased kidneys,  
298 we have previously shown that the enzyme  $\gamma$ -GT is preferentially expressed in the proximal  
299 tubules of injured kidneys and only marginally in the glomerulus (17). Therefore, in the ADR  
300 model, we used the already active amine-GSI metabolite which is not dependant on  $\gamma$ -GT  
301 enzymatic activation within the target organ. In the ADR experimental model as in the AA  
302 model, concomitant treatment with the amine-GSI metabolite was able to control proteinuria,  
303 but not weight loss (**Figure 7A**). ADR administration also induced Notch1 expression and  
304 genes of the RAS in the injured kidneys, which could to some extent be down-regulated by  
305 concomitant administration of the amine-GSI (**Figure 7B**). As compared to the AA model of  
306 severe tubulopathy, acute inflammatory pathway genes were not all consistently upregulated  
307 in this setting, which corresponded to a less acutely toxic and destructive effect of ADR on  
308 renal tissues; ADR mainly inducing progressive glomerular damage. **Figure 7C** indeed shows  
309 that ADR-mediated lesions are discrete on normal histology (light microscopy HE staining) at  
310 an early time-point, as ADR affects the glomerulus with no acute tubulointerstitial injury.

311 There is however a certain degree of glomerulosclerosis (fibrotic lesions are stained in blue in  
312 MTB sections, **Figure 7C lower panels**) in the absence of amine-GSI treatment. Finally,  
313 western blot analysis of kidney samples confirmed the modulation of Notch1 activation (as  
314 detected by its active cleaved form) upon administration of amine-GSI to ADR-treated mice  
315 (**Figure 7D**).

316

## 317 **Discussion**

318 Within the kidney, injury to tubular or glomerular cells is the initiating cause of acute and  
319 chronic diseases, leading to progressive dysfunction and end-stage renal failure. Inflammatory  
320 and non-inflammatory stresses affect the tubulointerstitial tissue and/or the glomerulus and  
321 lead to alterations in their structure, permeability and function. However, irrespective to the  
322 initial insult, disease progression ultimately leads to irreversible glomerulosclerosis,  
323 interstitial fibrosis and tubular atrophy. Recent studies of various renal diseases in humans  
324 and rodent experimental models have yielded several candidate pathways for therapy, which  
325 include the Notch pathway (3,6,7,14,22,30,31,40,43,47). In experimental mouse models,  
326 conditional overexpression of the active Notch1 protein in podocytes results in massive  
327 proteinuria and glomerulosclerosis, leading to renal failure and death of the animals. Genetic  
328 deletion of Notch transcriptional binding partners or treatment with  $\gamma$ -secretase inhibitors,  
329 preventing Notch activation and translocation to the nucleus, protected the animals from  
330 nephrotic syndrome. Thus, current data strongly suggest that targeted pharmacologic  
331 inhibition of the Notch signaling pathway may prevent kidney damage and improve organ  
332 survival.

333

334 Notch1-4 are transmembrane proteins that interact with ligands of the Jagged and Delta  
335 family. This interaction triggers a series of proteolytic cleavages within the cell. The final  $\gamma$ -  
336 secretase complex-mediated cleavage releases the NICD, which is a transcription factor. The  
337 function of Notch is context-dependent, regulating tissue homeostasis, cell differentiation and  
338 stem cell maintenance in adult life. Regulation of Notch pathway signaling mainly occurs at  
339 the levels of ligand binding and  $\gamma$ -secretase complex-mediated cleavage (20). We have  
340 previously shown that an N-Ac- $\gamma$ -Glu-GSI prodrug was selectively metabolized in the kidney  
341 after i.p. application to an amine-GSI metabolite displaying high Notch antagonism (17). Thus



342 in the present study, the potential beneficial nephroprotective effects of targeting Notch with  
343 these functionalized GSI-based prodrugs were investigated using two *in vivo* murine models.  
344 AA is a natural herbal component which is toxic to the renal tubular epithelial cells, leading to  
345 a dose-dependent rapidly progressive interstitial nephropathy and renal failure (5). AA acute  
346 tubular toxicity is a result of mitochondrial injury with defective activation of antioxidative  
347 enzymes leading to impaired regeneration, apoptosis and defective autophagy of proximal  
348 tubular epithelial cells, thus progressive tubular atrophy and interstitial fibrosis (37,50). ADR  
349 is an anticancer chemotherapeutic agent widely used in the clinic. ADR-induced nephropathy  
350 (10,23,29,32) is a well described rodent model of progressive glomerular disease, mediated by  
351 an oxidative stress and characterized by massive proteinuria due to podocyte injury, followed  
352 by glomerulosclerosis, tubulo-interstitial inflammation and fibrosis. ADR-induced renal  
353 injury has been shown in numerous studies to be modulated both by non-immune and immune  
354 factors. In the present study, we show that treatment with functionalized GSIs could alleviate  
355 proteinuria and slightly limit acute kidney dysfunction of mice exposed to AA or ADR. Gene  
356 expression profiles analysis of kidney sections demonstrated the induction of Notch1 and its  
357 downstream signalling, as well as a very high expression of the active cleaved form of Notch1  
358 by immunohistochemistry and western blot analysis of injured kidneys, which was reduced by  
359 concomitant treatment with the functionalized GSIs. However, although the administration of  
360 these GSIs could inhibit the activation of Notch and its downstream pathways, selectively  
361 blocking Notch activation in the kidney proved insufficient to prevent acute renal failure due  
362 to severe tubulointerstitial or glomerular injury, such as induced in our models.

363

364 Following Notch activation mediated by the transmembrane  $\gamma$ -secretase complex, the released  
365 NICD translocates to the nucleus where it interacts with transcription factors and histone  
366 acyltransferases (8,35,46). Nuclear localization of the NICD promotes the transcription of

367 Notch-dependent target genes in a context- and cell-dependent manner. Several studies  
368 conducted to identify genes regulated by Notch have demonstrated that these responsive  
369 genes include *Notch* itself, *HES1*, *Snail*, *Nephrin*, *CDK2* and genes involved in pro-  
370 inflammatory pathways (13,18,24,26,34,38,39,41,49). In mice, a loss of the slit diaphragm  
371 protein Nephrin was observed exclusively in podocytes expressing activated Notch.  
372 Overexpression of activated Notch decreased cell surface Nephrin and increased cytoplasmic  
373 Nephrin in transfected HEK 293 cells. Thus, Notch signaling induces endocytosis of Nephrin,  
374 thereby triggering the onset of proteinuria (44). Notch signaling has been shown to be  
375 associated with inflammatory diseases (1,11,14). The pro-inflammatory cytokine IL-6 has  
376 also been shown to be regulated by Notch signaling and controlled by p53 and the NFκB  
377 pathway (11,15). A complex signaling crosstalk has also been described in cardiovascular  
378 diseases where inflammatory responses regulate Notch signaling and reciprocally Notch has a  
379 functional role on inflammatory processes (36). Overall, Notch signaling has a role in  
380 controlling the cell cycle via CDK2, cell differentiation and transcription via HES1, cell  
381 adhesion and epithelial-to-mesenchymal transdifferentiation (EMT) via Snail and Nephrin, as  
382 well as the immune response via the cytokines IL-1β, IL-6 and the NFκB pathway. In the  
383 present report, quantitative real-time PCRs performed on mRNAs extracted from the acutely  
384 injured kidneys demonstrated an upregulation of the expression of down-stream genes of the  
385 Notch pathway, including *Notch1*, *HES1*, *Snail* and *CDK2*, and of *IL-1β* and *IL-6* likely  
386 mediated by the NFκB pathway, which could all be selectively down-regulated upon  
387 administration to the AA and ADR-exposed animals of the functionalized GSIs.

388

389 The renin-angiotensin system (RAS) is a main contributor in the regulation of kidney function  
390 in homeostatic and disease conditions, acting independently in the blood and the kidney  
391 (12,42). All the RAS components have been found in the kidney, differentially expressed in

392 various renal compartments. Conversion by APA, a membrane-bound zinc-dependent  
393 aminopeptidase expressed in renal proximal tubules and in glomerular cells and which is  
394 upregulated upon tissue injury (17), of Ang II to Ang III was shown to be critical for  
395 angiotensin-mediated effects in the kidney (19,27,28,33). The AT1 and AT2 receptors display  
396 opposing functions and selectivity for Ang II and Ang III (4,33). In the intact kidney the Ang  
397 II/AT1R axis is the more highly expressed, whereas in diseased conditions the Ang III/AT2R  
398 axis may represent a physiological response to renal tissue stress. Previous data suggest a  
399 crosstalk between Ang II and the activation of the Notch pathway in the development of renal  
400 diseases. Ang II was shown to induce the synthesis by murine podocytes of extracellular  
401 matrix components and transforming growth factor (TGF)- $\beta$ 1 that could be inhibited by GSIs  
402 (48). In isolated perfused rat kidneys and cultured human podocytes, Ang II down-regulated  
403 Nephlin expression via Notch1 activation and nuclear translocation of Snail. HES1 is a  
404 Notch1-downstream transcription factor that was shown to activate Snail in cultured  
405 podocytes. Changes of the Snail/Nephlin axis in patients with advanced diabetic nephropathy  
406 were normalized by pharmacological inhibition of the RAS. Overall, these data point to the  
407 relevant role of Ang II in promoting glomerular injury via activation of Notch1/Snail  
408 signaling in podocytes, resulting in the down-regulation of Nephlin expression, the integrity  
409 of which is crucial for the glomerular filtration barrier (9). Therefore, our observation in the  
410 present report of a link between targeted blockade of the Notch pathway, inflammatory stress  
411 responses and the RAS opens new therapeutic implications for the treatment of kidney  
412 diseases, suggesting that the addition of drugs able to control Notch activation such as  
413 functionalized GSIs may be of therapeutic value.

414

415

416

417 **Abbreviations**

418 Ac: acetyl

419 AA: aristolochic acid; 8-methoxy-6-nitrophenanthro[3,4-*d*][1,3]dioxole-5-carboxylic acid

420 ADR: Adriamycin

421 Ang: angiotensin

422 APA: glutamyl aminopeptidase (EC 3.4.11.7.)

423 AT1/2: angiotensin receptor type 1 or type 2

424  $\gamma$ -GT:  $\gamma$ -glutamyl-transpeptidase (EC 2.3.2.2.)

425 RAS: renin-angiotensin system

426  $\gamma$ -GCT:  $\gamma$ -glutamylcyclotransferase (EC 2.3.2.4.)

427

428 **Acknowledgements**

429 We thank Helmut Jacobsen and Karlheinz Bauman for supporting our project. We thank also  
430 Susanne Mohr, Maria Cristina De Vera Mudry, Claudine Sarron-Petit and Marco Zihlman for  
431 measuring and analyzing plasma toxicology markers; Jean-Christophe Stehle for his expert  
432 help in immunohistochemistry. This work was supported by the CHUV and F. Hoffmann-La  
433 Roche. JCW thanks F. Hoffmann-La Roche for support by the Roche Postdoc Fellowship  
434 program. DG is supported by Fondation Pierre Mercier pour la Science, Fondation Medi-CAL  
435 Futur and Fondation Lausannoise pour la Transplantation d'Organes.

436

437 **Conflicts of interest**

438 MS and JDA are employees of F. Hoffmann-La Roche but declare no conflict of interest.

439 JCW, RK, JM, LJJ and DG declare no conflict of interest.

440

441 **References**

- 442 **1. Andersen P, Uosaki H, Shenje LT, Kwon C.** Non-canonical Notch signaling:  
443 emerging role and mechanism. *Trends Cell Biol* 22: 257-265, 2012.
- 444
- 445 **2. Baudoux TE, Pozdzik AA, Arlt VM, De Prez EG, Antoine MH, Quellard N,**  
446 **Goujon JM, Nortier JL.** Probenecid prevents acute tubular necrosis in a mouse model of  
447 aristolochic acid nephropathy. *Kidney Int* 82(10):1105-13, 2012.
- 448
- 449 **3. Bielez B, Sirin Y, Si H, Niranjana T, Gruenwald A, Ahn S, Kato H, Pullman J,**  
450 **Gessler M, Haase VH, Susztak K.** Epithelial Notch signaling regulates interstitial fibrosis  
451 development in the kidneys of mice and humans. *J Clin Invest* 120: 4040-4054, 2010.
- 452
- 453 **4. Carey RM, Padia SH.** Role of angiotensin AT<sub>2</sub> receptors in natriuresis: intrarenal  
454 mechanisms and therapeutic potential. *Clin Exp Pharm Physiol* 40: 527-534, 2013.
- 455
- 456 **5. Debelle FD, Nortier JL, De Prez EG, Garbar CH, Vienne AR, Salmon**  
457 **IJ, Deschodt-Lanckman MM, Vanherweghem JL.** Aristolochic acids induce chronic renal  
458 failure with interstitial fibrosis in salt-depleted rats. *J Am Soc Nephrol* 13(2):431-6, 2002.
- 459
- 460 **6. Djudjaj S, Chatziantoniou C, Rafftseder U, Guerrot D, Dussaule JC, Boor P,**  
461 **Kerroch M, Hanssen L, Brandt SM, Dittrich A, Ostendorf T, Floege J, Zhu C,**  
462 **Lindenmeyer M, Cohen CD, Mertens PR.** Notch-3 receptor activation drives inflammation  
463 and fibrosis following tubule-interstitial kidney injury. *J Pathol* 228: 286-299, 2012.
- 464
- 465 **7. Dressler GR.** Another niche for Notch. *Kidney Int* 73: 1207-1209, 2008.

466

467 **8. Fortini, M. E.; Artavanis-Tsakonas, S.** The suppressor of hairless protein  
468 participates in Notch receptor signaling. *Cell* 79: 273-282, 1994.

469

470 **9. Gagliardini E, Perico N, Rizzo R, Buelli S, Longaretti L, Perico L, Tomasoni S,**  
471 **Zoja C, Macconi D, Morigi M, Remuzzi G, Benigni A.** Angiotensin II contributes to  
472 diabetic renal dysfunction in rodents and humans via Notch1/Snail pathway. *Am J Pathol* 183:  
473 119–130, 2013.

474

475 **10. Gao K, Chi Y, Sun W, Takeda M, Yao J.** 5'-AMP-activated protein kinase  
476 attenuates adriamycin-induced oxidative podocyte injury through thioredoxin-mediated  
477 suppression of the apoptosis signal-regulating kinase 1-p38 signaling pathway. *Mol*  
478 *Pharmacol* 85: 460-471, 2014.

479

480 **11. Gentle ME, Rose A, Bugeon L, Dallman MJ.** Noncanonical Notch signaling  
481 modulates cytokine responses of dendritic cells to inflammatory stimuli. *J Immunol* 189:  
482 1274-1284, 2012.

483

484 **12. Grobe N, Elased KM, Cool DR, Morris M.** Mass spectrometry for the molecular  
485 imaging of angiotensin metabolism in kidney. *Am J Physiol Endocrinol Metab* 302: E1016–  
486 E1024, 2012.

487

488 **13. Hamidi H, Gustafson D, Pellegrini M, Gasson J.** Identification of novel targets of  
489 CSL-dependent Notch signaling in hematopoiesis. *PloS One* 6: e20022, 2011.

490

- 491 **14. Heitzler P.** Biodiversity and noncanonical Notch signaling. *Curr Top Dev Biol* 92:  
492 457-481, 2012.  
493
- 494 **15. Jin S, Mutvei AP, Chivukula IV, Andersson ER, Ramsköld D, Sandberg R, Lee**  
495 **KL, Kronqvist P, Mamaeva V, Östling P, Mpindi JP, Kallioniemi O, Screpanti I,**  
496 **Poellinger L, Sahlgren C, Lendahl,U.** Non-canonical Notch signaling activates IL-  
497 6/JAK/STAT signaling in breast tumor cells and is controlled by p53 and IKKalpha/IKKbeta.  
498 *Oncogene* 32: 4892-4902, 2013.  
499
- 500 **16. Juillerat-Jeanneret L, Monnet-Tschudi F, Zürich MG, Lohm S, Duijvestijn AM,**  
501 **Honegger P.** Regulation of peptidase activity in a three-dimensional aggregate model of brain  
502 tumor vasculature. *Cell Tissue Res* 311: 53-59, 2003.  
503
- 504 **17. Juillerat-Jeanneret L, Flohr A, Schneider M, Walter, I, Wyss J C, Kumar R,**  
505 **Golshayan D, Aebi J D.** Targeted  $\gamma$ -Secretase Inhibition to Control the Notch Pathway in  
506 Renal Diseases. *J Med Chem* 58: 8097-8109, 2015.  
507
- 508 **18. Kao HY, Ordentlich P, Koyano-Nakagawa N, Tang Z, Downes M, Kintner CR,**  
509 **Evans RM, Kadesch T.** A histone deacetylase corepressor complex regulates the Notch  
510 signal transduction pathway. *Genes Dev* 12: 2269-2277, 1998.  
511
- 512 **19. Kemp BA, Bell JF, Rottkamp DM, Howell NL, Shao W, Navar G, Padia SH,**  
513 **Carey RM.** Intrarenal angiotensin III is the predominant agonist for proximal tubules  
514 angiotensin type 2 receptors. *Hypertension* 60: 387-395, 2012.  
515

- 516 **20. Kumar R, Juillerat-Jeanneret L, Golshayan D.** Notch antagonists: potential  
517 modulators of cancer and inflammatory diseases. *J Med Chem* 59:7719-7737,2016.  
518
- 519 **21. Lambers Heerspink HJ, de Zeeuw D.** Novel drugs and interventions strategies for  
520 the treatment of chronic kidney disease. *Br J Clin Pharm* 76: 536-550, 2013.  
521
- 522 **22. Lasagni L, Ballerini L, Angelotti ML, Parente E, Sagrinati C, Mazzinghi B,**  
523 **Peired A, Ronconi E, Becherucci F, Bani D, Gacci M, Carini M, Lazzeri E, Romagnani**  
524 **P.** Notch activation differentially regulates renal progenitor proliferation and differentiation  
525 toward the podocyte lineage in glomerular disorders. *Stem Cells* 28: 1673-1685, 2010.  
526
- 527 **23. Lee VW, Harris DC.** Adriamycin nephropathy: a model of focal segmental  
528 glomerulosclerosis. *Nephrology* 16: 30-38, 2011.  
529
- 530 **24. Lipsey CC, Harbuzariu A, Daley-Brown D, Gonzalez-Perez RR.** Oncogenic role of  
531 leptin and Notch interleukin-1 leptin crosstalk outcome in cancer. *World J Methodol* 6: 43-55,  
532 2016.  
533
- 534 **25. Livak KJ, Schmittgen TD.** Analysis of relative gene expression data using real-time  
535 quantitative PCR and the  $2^{-\Delta\Delta C(T)}$  *Method Methods* 25: 402–408, 2001.  
536
- 537 **26. Lobry C, Oh P, Mansour MR, Look AT, Aifantis, I.** Notch signaling: switching an  
538 oncogene to a tumor suppressor. *Blood* 123: 2451-2459, 2014.  
539
- 540 **27. Mentzel S, Assmann KJ, Dijkman HB, de Jong AS, van Son JPHF, Wetzels JFM,**



- 541 **Koene RAP.** Inhibition of aminopeptidase A activity causes acute albuminuria in mice: and  
542 angiotensin II-mediated effect? *Nephrol Dial Transplant* 11: 2163-2169, 1996.
- 543
- 544 **28. Mentzel S, Van Son JP, De Jong AS, H B Dijkman HB, R A Koene RA, J F**  
545 **Wetzels JF, Assmann KJ.** Mouse glomerular epithelial cells in culture with features of  
546 podocytes in vivo express aminopeptidase A and angiotensinogen but not other components  
547 of the renin-angiotensin system. *J Am Soc Nephrol* 8: 706-719, 1997.
- 548
- 549 **29. Mukhopadhyay P, Rajesh M, Batkai S, Kashiwaya Y, Haskó G, Liaudet L, Szabó**  
550 **C, Pacher P.** Role of superoxide, nitric oxide, and peroxynitrite in doxorubicin-induced cell  
551 death in vivo and in vitro. *Am J Physiol Heart Circ Physiol* 296: H1466-H1483, 2009.
- 552
- 553 **30. Nath KA.** Tubulointerstitial changes as a major determinant in the progression of  
554 renal damage. *Am J Kidney Dis* 20: 1-17, 1992.
- 555
- 556 **31. Niranjana T, Murea M, Susztak K.** The pathogenic role of Notch activation in  
557 podocytes. *Nephron Exp Nephrol.* 111: e73-79, 2009.
- 558
- 559 **32. Okuda S, Oh Y, Tsuruda H, Onoyama K, Fujimi S, Fujishima M.** Adriamycin-  
560 induced nephropathy as a model of chronic progressive glomerular disease. *Kidney Int* 29:  
561 502-510, 1986.
- 562
- 563 **33. Padia SH, Kemp BA, Howell NL, Fournie-Zaluski MC, Roques BP, Carey RM.**  
564 Conversion of renal angiotensin II to angiotensin III is critical for AT<sub>2</sub> receptor-mediated  
565 natriuresis in rats. *Hypertension* 51: 460-465, 2008.

- 566
- 567 **34. Palomero T, Lim WK, Odom DT, Sulis ML, Real PJ, Margolin A, Barnes KC,**  
568 **O'Neil J, Neuberg D, Weng AP, Aster JC, Sigaux F, Soulier J, Look AT, Young RA,**  
569 **Califano A, Ferrando A.** NOTCH1 directly regulates c-MYC and activates a feed-forward-  
570 loop transcriptional network promoting leukemic cell growth. *Proc Nat Acad Sci, USA* 103:  
571 18261-18266, 2006.
- 572
- 573 **35. Petcherski AG, Kimble J.** Mastermind is a putative activator for Notch. *Curr Biol* 10:  
574 471-473, 2000.
- 575
- 576 **36. Quillard T, Charreau B.** Impact of Notch signaling on inflammatory responses in  
577 cardiovascular disorders. *Int J Mol Sci* 14: 6863–6888, 2013.
- 578
- 579 **37. Romanov V, Whyard T, Bonala R, Johnson F, Grollman A.** Glutamate  
580 dehydrogenase requirement for apoptosis induced by aristolochic acid in renal tubular  
581 epithelial cells. *Apoptosis* 16: 1217-1228, 2011.
- 582
- 583 **38. Ronchini C, Capobianco AJ.** Induction of cyclin D1 transcription and CDK2 activity  
584 by Notch(ic): implication for cell cycle disruption in transformation by Notch(ic). *Mol Cell*  
585 *Biol* 21: 5925-5934, 2001.
- 586
- 587 **39. Saad S, Stanners SR, Yong R, Tang O, Pollock CA.** Notch mediated epithelial to  
588 mesenchymal transformation is associated with increased expression of the Snail transcription  
589 factor. *Int J Biochem Cell Biol* 42:1115-1122, 2010.
- 590

- 591 **40. Sanchez-Nino MD, Ortiz A.** Notch3 and kidney injury: never two without three. *J*  
592 *Pathol* 228: 266-273, 2012.
- 593
- 594 **41. Shawber C, Nofziger D, Hsieh JJ, Lindsell C, Bogler O, Hayward D, Weinmaster**  
595 **G.** Notch signaling inhibits muscle cell differentiation through a CBF1-independent pathway.  
596 *Development* 122: 3765-3773, 1996.
- 597
- 598 **42. Sparks MA, Crowley SD, Gurley SB, Mirotso M, Coffman TM.** Classical renin-  
599 angiotensin system in kidney physiology. *Compr Physiol* 4, 1201–1228, 2014.
- 600
- 601 **43. Thomas MC, Groop PH.** New approaches to the treatment of nephropathy in  
602 diabetes. *Exp Opin Invest Drugs* 20: 1057-1071, 2011.
- 603
- 604 **44. Waters AM, Wu MY, Huang YW, Liu GY, Holmyard D, Onay T, Jones N, Egan**  
605 **SE, Robinson LA, Piscione TD.** Notch promotes dynamin-dependent endocytosis of nephrin.  
606 *J Am Soc Nephrol* 23: 27-35, 2012.
- 607
- 608 **45. Wolfe MS.** The  $\gamma$ -secretase complex: membrane-embedded proteolytic ensemble.  
609 *Biochemistry* 45: 7931-7939, 2006.
- 610
- 611 **46. Wu L, Aster JC, Blacklow SC, Lake R, Artavanis-Tsakonas S, Griffin JD.**  
612 MAML1, a human homologue of *Drosophila* mastermind, is a transcriptional co-activator for  
613 NOTCH receptors. *Nature Gen* 26: 484-489, 2000.
- 614
- 615 **47. Xiao Z, Zhang J, Peng X, Dong Y, Jia L, Li H, Du J.** The Notch- $\gamma$ -secretase

616 inhibitor ameliorates kidney fibrosis via inhibition of TGF- $\beta$ /Smad2/3 signaling pathway  
617 activation. *Int J Biochem Cell Biol* 55: 65-71, 2014.

618

619 **48. Yao M, Wang X, Wang X, Zhang T, Chi Y, Gao F.** The Notch pathway mediates  
620 the angiotensin II-induced synthesis of extracellular matrix components in podocytes. *Int J*  
621 *Mol Med* 36: 294-300, 2015.

622

623 **49. Zanotti S, Canalis E.** Interleukin 6 mediates selected effects of Notch in  
624 chondrocytes. *Osteoarthritis Cartilage* 21: 1766-1773, 2013.

625

626 **50. Zeng Y, Li S, Wu J, Chen W, Sun H, Peng W.** Autophagy inhibitors promoted  
627 aristolochic acid I induced renal tubular epithelial cell apoptosis via mitochondrial pathway,  
628 but alleviated nonapoptotic cell death in mouse acute aristolochic acid nephropathy model.  
629 *Apoptosis* 19: 1215-1224, 2014.

630

631

632

633

634

635 **Tables**

636

637 **Table 1. Sequences of the primers used for the qPCR experiments.**

<i>gene symbol</i>	<i>forward sequence (5'–3')</i>	<i>reverse sequence (5'–3')</i>
<i>AGT</i>	GGCAAATCTGAACAACATTGG	TTCCTCCTCTCCTGCTTTGA
<i>APA</i>	TGGACTCCAAAGCTGATCCT	TCAGCCCATCTGACTGGAAT
<i>AT1</i>	ACTCACAGCAACCCTCCAAG	CTCAGACACTGTTCAAAATGCAC
<i>CDK2</i>	TTCCTCTTCCCCTCATCAAG	ACGGTGAGAATGGCAGAAAG
<i>Gapdh</i>	GTCGGTGTGAACGGATTTG	AAGATGGTGATGGGCTTCC
<i>HES1</i>	TGCCAGCTGATATAATGGAGAA	CCATGATAGGCTTTGATGACTTT
<i>IL-1<math>\beta</math></i>	GGCCTCAAAGGAAAGAATC	CTCTGCTTGTGAGGTGCTGA
<i>IL-6</i>	AGAAGGGCCTGGAATGAAAC	AAGACCCTGCTGGAACAAGA
<i>Nephrin1</i>	GGATATAGTCTGCACCGTCGAT	TCAGTTCCTCCTCGTCTTCC
<i>NF<math>\kappa</math>B1</i>	GGGTCTGGGGATACTGAACA	GCCTCCATCAGCTCTTTGAT
<i>NF<math>\kappa</math>B2</i>	TGGAACAGCCCAAACAGC	CACCTGGCAAACCTCCAT
<i>Notch1</i>	CTGGACCCCATGGACATC	AGGATGACTGCACACATTGC
<i>Renin</i>	GGAGGAAGTGTTCTCTGTCTACTACA	GCTACCTCCTAGCACACCTC
<i>Snail</i>	CTTGTGTCTGCACGACCTGT	CAGGAGAATGGCTTCTCACC

638

639

640 **Table 2. Serum chemistry profile of mice exposed to aristolochic acid (AA) alone, or with**  
 641 **the N-Ac- $\gamma$ -Glu-GSI or the amine-GSI.**

642

		<i>Creat</i>	<i>Urea</i>	<i>Prot</i>	<i>Alb</i>	<i>ASAT</i>	<i>ALAT</i>	<i>AlkP</i>
		$\mu\text{mol/l}$	$\text{mmol/l}$	$\text{g/l}$	$\text{g/l}$	$\text{U/l}$	$\text{U/l}$	$\text{U/l}$
<b>Control</b>	mean	43.4	8.8	53.4	30.7	372.0	55.6	141.5
	$\pm$ sd	4.8	1.1	3.2	2.5	77.6	4.2	11.5
<b>N-Ac-<math>\gamma</math>-Glu-GSI</b>		37.4	7.7	54.0	30.8	516.0	92.4	136.1
<b>AA</b>		4.0	0.5	2.5	1.3	212.1	26.3	18.1
		251.4	112.3	52.2	29.4	459.4	179.8	108.7
<b>AA +</b>		69.0	15.6	4.7	3.0	204.6	73.8	27.8
		160.3	85.2	46.8	26.3	375.9	43.4	94.6
<b>N-Ac-<math>\gamma</math>-Glu-GSI</b>		69.3	20.5	15.1	8.1	120.4	16.8	25.6
<b>AA +</b>		169.0	90.0	57.6	31.0	550.6	208.8	140.0
<b>amine-GSI</b>		29.3	9.8	2.4	2.8	219.6	83.5	20.3

643

644 *Abbreviations:* Creat: creatinine; Prot: proteins; Alb: albumin; ASAT: aspartate aminotransferase; ALAT:  
 645 alanine aminotransferase; AlkP: alkaline phosphatase.

646

647

648

649

650

651 **Figures Legends**

652 **Figure 1. Chemical structure of the N-Ac- $\gamma$ -Glu-GSI prodrug and its proteolytic activation.**

653 The prodrug is composed of the active compound ( $\gamma$ -secretase inhibitor, GSI), a linker  
654 (amine) and the targeting N-acetyl (N-Ac)- $\gamma$ -Glu-moiety as substrate for the releasing acylase  
655 and  $\gamma$ -Glu-transpeptidase ( $\gamma$ -GT) and/or  $\gamma$ -Glu-cyclotransferase peptidases  $\gamma$ -GCT (arrows).

656

657 **Figure 2. Body weight (A) and proteinuria (B) of mice exposed to aristolochic acid, N-Ac- $\gamma$ -**  
658 **Glu-GSI, aristolochic acid together with N-Ac- $\gamma$ -Glu-GSI and aristolochic acid with amine-**  
659 **GSI.**

660 Acute tubular injury was induced in 10 weeks old BALB/c male mice by i.p. injection of  
661 aristolochic acid (AA). The GSI analogs were administered i.p., starting one day before  
662 injection of AA (day -1) and then twice daily until day 6 evening. The animals were  
663 monitored clinically daily, weighted and the level of albuminuria was semi-quantitatively  
664 assessed at day 0, day 3 and day 6. Results are presented as means  $\pm$  sd for all mice in each  
665 experimental group, with comparisons between treated *versus* control animals or between  
666 treatments. (\*\*p<0.01; \*\*\*p<0.001; NS not statistically significant).

667

668 **Figure 3. Histology of the kidneys and livers of mice treated with aristolochic acid and the**  
669 **N-Ac- $\gamma$ -Glu-GSI.**

670 Acute kidney injury was induced by i.p. injection of aristolochic acid (AA) (1x5mg/kg) in 10  
671 weeks old BALB/c male mice. Hematoxylin/eosin (HE), Masson's trichrome blue (MTB) and  
672  $\alpha$ -smooth muscle actin ( $\alpha$ -SMA) staining of mouse kidney sections (A) and MTB staining of  
673 liver sections (B) of untreated (controls), mice treated with N-Ac- $\gamma$ -Glu-GSI, or after  
674 exposure to AA without or with N-Ac- $\gamma$ -Glu-GSI treatment. Representative  
675 images/experimental groups are shown (40x).

676 **Figure 4. Expression of Notch1 and cleaved Notch1 in the kidneys of mice treated with**  
677 **aristolochic acid and N-Ac- $\gamma$ -Glu-GSI.**

678 (A) Frozen kidneys sections (7 $\mu$ m) of control and aristolochic acid (AA)-treated mice,  
679 without or with the N-Ac- $\gamma$ -Glu-GSI, were exposed to either anti-Notch1 or anti-cleaved  
680 Notch1 antibodies, followed by the alkaline phosphatase-fast-red chromogen staining and  
681 hematoxylin counterstaining. Immunostaining is visualized as a red-brown precipitate. (B)  
682 Western blot analysis of cleaved Notch1 expression in kidney samples from control and AA-  
683 treated mice, without or with the N-Ac- $\gamma$ -Glu-GSI. Results of 3 representative  
684 mice/experimental group are shown. GAPDH was used as loading control and the intensities  
685 of the bands were quantified relative to GAPDH.

686

687 **Figure 5. Notch1 and inflammatory pathway-responsive genes in the kidneys of mice**  
688 **exposed to aristolochic acid and the N-Ac- $\gamma$ -Glu-GSI.**

689 Acute kidney injury was induced by i.p. injection of aristolochic acid (AA) in 10 weeks old  
690 BALB/c male mice. At the end of the experiment (day 7 morning), the animals were  
691 sacrificed and mRNAs were extracted from the snap-frozen kidneys. The levels of expression  
692 of the mRNAs for (A) Notch1-responsive genes and (B) Notch1-inducible inflammatory  
693 markers were quantified by qRT-PCR and results were averaged for all animals in each  
694 experimental group. Results are presented as % of changes in the mRNA levels in the treated  
695 animals *versus* control animals  $\pm$  sem. (\*p<0.05; \*\*p<0.01; \*\*\*p<0.001). C.  
696 Immunohistochemistry staining of NF $\kappa$ B p65 on kidney sections of untreated (controls),  
697 control mice treated with N-Ac- $\gamma$ -Glu-GSI, or after exposure to AA without or with N-Ac- $\gamma$ -  
698 Glu-GSI treatment.

699

700 **Figure 6. Modulation of genes of the renin-angiotensin system (RAS) in the kidneys of**



701 *mice administered aristolochic acid and treated with functionalized GSIs.*

702 After 7 days of treatment, with either (A) aristolochic acid (AA) alone or together with N-Ac-  
703  $\gamma$ -Glu-GSI or (B) AA alone or with amine-GSI, the animals were sacrificed and their kidneys  
704 extracted for the determination by qRT-PCR of the mRNA levels of genes of the components  
705 of the RAS. Results were averaged for all animals per experimental group and are presented  
706 as % of changes in the mRNA levels in the treated animals *versus* control animals  $\pm$  sem.  
707 (\* $p < 0.05$ ; \*\* $p < 0.01$ ; \*\*\* $p < 0.001$ ).

708

709 **Figure 7. Clinical parameters, Notch1-related pathways activation profiles and kidney**  
710 **histology of mice exposed to adriamycin and the amine-GSI.**

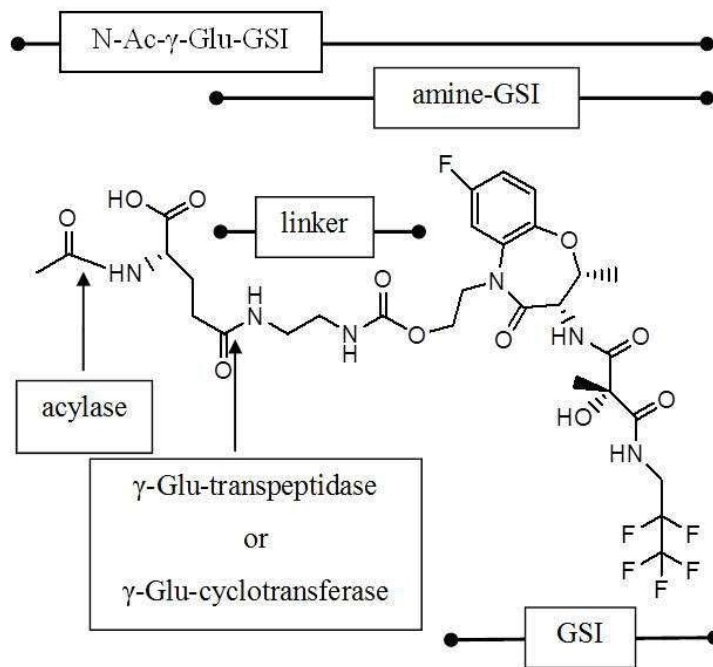
711 Glomerular injury was induced in 10 weeks old BALB/c male mice by i.p. injection of  
712 adriamycin (ADR). The amine-GSI metabolite was administered i.p., starting one day before  
713 injection of ADR (day -1) and then twice daily until day 6 evening. (A) Mice were monitored  
714 clinically daily, weighted and the level of proteinuria was semi-quantitatively assessed at day  
715 0, day 3 and day 6. Results were averaged for all mice per experimental group and means  $\pm$  sd  
716 are shown. (B) After 7 days of treatment, with either ADR alone or together with amine-GSI,  
717 the animals were sacrificed and mRNAs were extracted from the snap-frozen kidneys. The  
718 levels of expression of the mRNAs for the Notch1-inducible genes and genes of the renin-  
719 angiotensin system (RAS) were quantified by qRT-PCR. Results were averaged for all  
720 animals per experimental group and are presented as % of changes in the mRNA levels in the  
721 treated animals *versus* the control animals  $\pm$  sem. (\* $p < 0.05$ ; \*\* $p < 0.01$ ; \*\*\* $p < 0.001$ ). (C)  
722 Kidney sections histology with hematoxylin/eosin (HE) and Masson's trichrome blue (MTB)  
723 stainings after ADR administration, alone or with amine-GSI. (D) Western blot analysis of  
724 cleaved Notch1 expression in kidney samples from control and ADR-treated mice, without or  
725 with the amine-GSI. Results of 3 representative mice/experimental group are shown. GAPDH

726 was used as loading control and the intensities of the bands were quantified relative to  
727 GAPDH.

728

## Figures

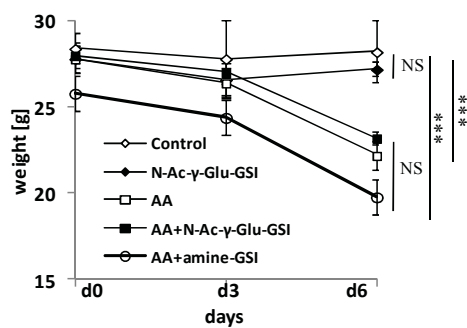
Figure 1.



Acylase and  $\gamma$ -Glu-cyclotransferase ( $\gamma$ -GCT) are cytoplasmic proteins,  $\gamma$ -Glu-transpeptidase ( $\gamma$ -GT) is a membrane-bound protein.

Figure 2.

A.



B.

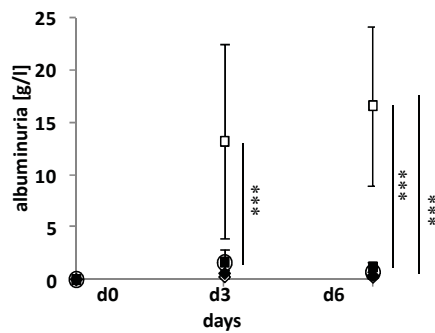
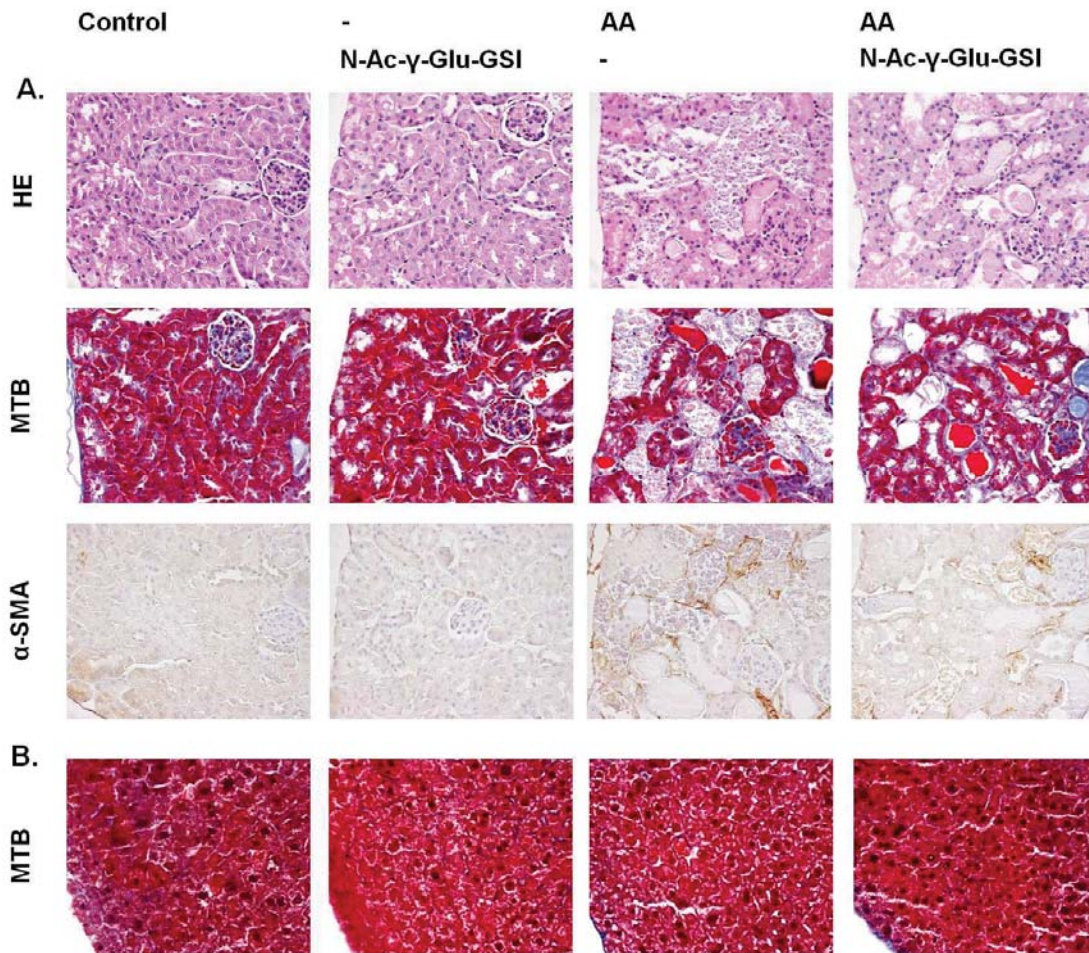


Figure 3.



**Figure 4.**

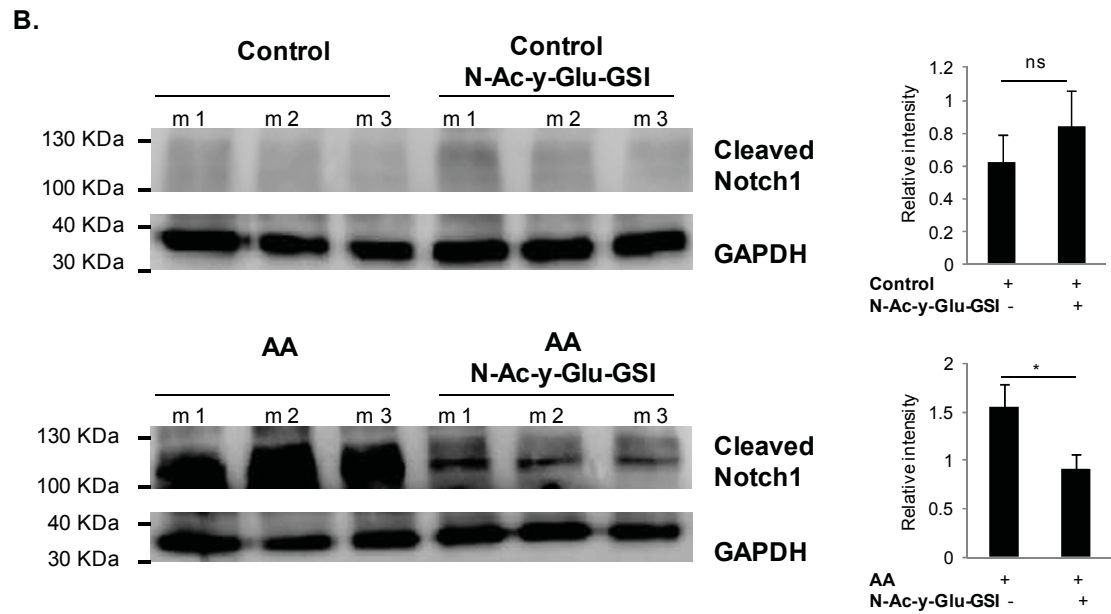
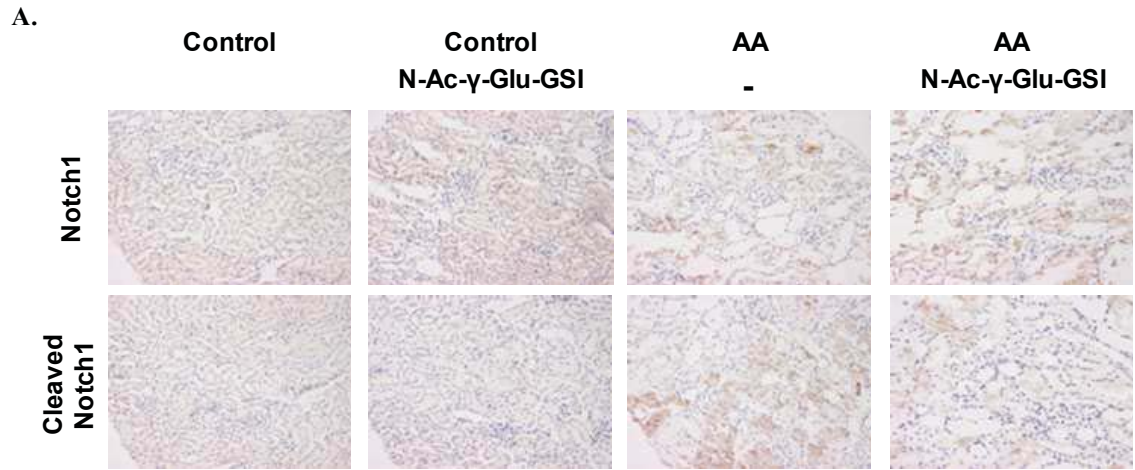
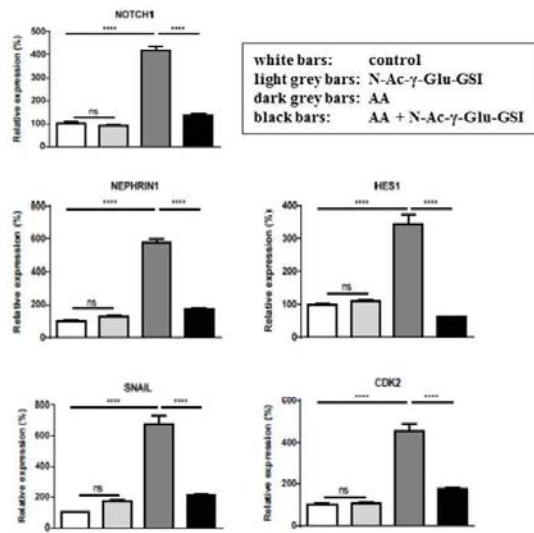
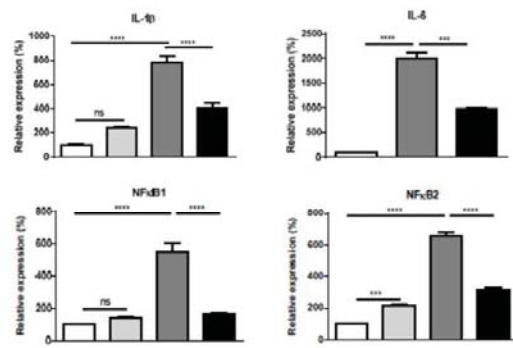


Figure 5.

**A. Notch-responsive genes**



**B. Inflammatory mediators**



**C. Control**

-  
N-Ac- $\gamma$ -Glu-GSI

AA

-

AA

N-Ac- $\gamma$ -Glu-GSI

NF $\kappa$ B p65

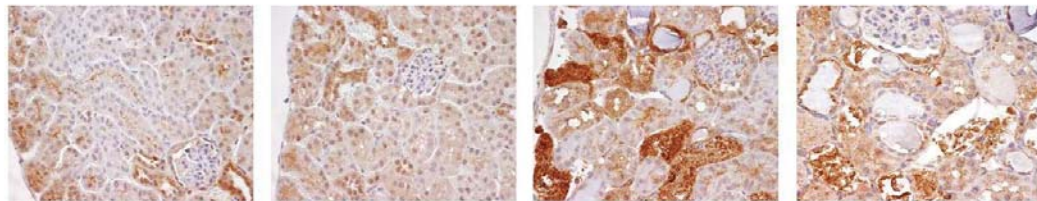
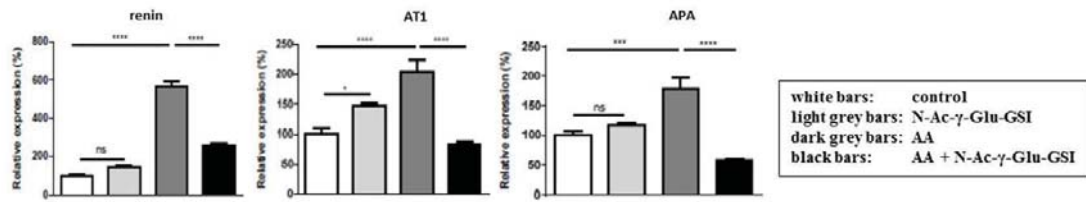
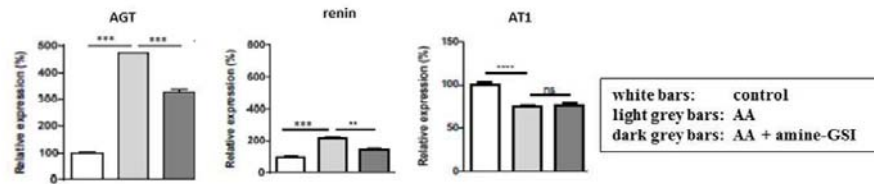


Figure 6.

A. AA and N-Ac- $\gamma$ -Glu-GSI



B. AA and amine-GSI





**Figure 7.**

